SPE 79709

A Comparison of Techniques for Coupling Porous Flow and Geomechanics

Rick H. Dean, SPE, and Xiuli Gai, University of Texas at Austin, Charles M. Stone, Sandia National Laboratories, and Susan E. Minkoff, University of Maryland, Baltimore County

This paper was prepared for presentation at the SPE Reservoir Simulation Symposium held in Houston, Texas, U.S.A., 3–5 February 2003.

Abstract

This paper compares three techniques for coupling multiphase porous flow and geomechanics. Sample simulations are presented to highlight the similarities and differences in the techniques. One technique uses an explicit algorithm to couple porous flow and displacements where flow calculations are performed every time step and displacements are calculated only during selected time steps. A second technique uses an iteratively coupled algorithm where flow calculations and displacement calculations are performed sequentially for nonlinear iterations during time steps. The third technique uses a fully coupled approach where the program's linear solver must solve simultaneously for fluid flow variables and displacement variables. The techniques for coupling porous flow with displacements are described, and comparison problems are presented for single-phase and three-phase flow problems involving poroelastic deformations. All problems in this paper are described in detail so the results presented here may be used for comparison with other geomechanical/porous flow simulators.

Introduction

Many applications in the petroleum industry require both an understanding of the porous flow of reservoir fluids and an understanding of reservoir stresses and displacements. Examples of such processes include subsidence, compaction drive, wellbore stability, sand production, cavity generation, high-pressure breakdown, well surging, thermal fracturing, fault activation, and reservoir failure involving pore collapse or solids disposal. It would be useful to compare porous flow/geomechanics techniques for all of these processes, since some of these processes involve a stronger coupling between porous flow and geomechanics than others. However, this paper looks at a subset of these processes and compares three coupling techniques for problems involving subsidence and compaction drive. All of the sample problems presented in this paper assume that the reservoir absolute permeabilities are constant during a run. Displacements influence fluid flow through calculation of pore volumes and fluid pressures enter the displacement calculations through the poroelastic constitutive equations.

Several authors have presented formulations for modeling poroelastic, multiphase flow. Settari and Walters[1] discuss the different methods that have been used to combine poroelastic calculations with porous flow calculations. They categorize these different methods of coupling poroelastic calculations with porous flow calculations as decoupled,[1] explicitly coupled, iteratively coupled, and fully coupled. The techniques discussed in this paper are explicitly coupled, iteratively coupled, and fully coupled.

For an explicitly coupled approach,[2-4] a simulator performs computations for multiphase porous flow each time step and performs geomechanical calculations for displacements during selected time steps. The frequency of geomechanical updates is driven by the magnitude of the pore volume changes during the time steps. If the pore volumes change slowly during time steps then few geomechanical updates are required. The ability to perform geomechanical calculations for selected time steps is a very attractive feature of the explicitly coupled approach because a major portion of the computational time for a porous flow/geomechanics run is often spent in calculating displacements. Another attractive feature of the explicitly coupled approach is that it is very straightforward to use this technique to couple an existing porous flow simulator with an existing geomechanics simulator. One shortcoming of the explicitly coupled approach is that the explicit nature of the coupling can impose time step restrictions on runs because of concerns about stability and accuracy. However, for many subsidence problems the fluid flow calculations require time steps that are smaller than those imposed by the explicit coupling calculations.

For the iteratively coupled approach, multiphase porous flow and displacements are coupled through the nonlinear iterations for each time step. During each nonlinear iteration, a simulator performs computations sequentially for multiphase porous flow and for displacements. The flow and displacement calculations are then coupled through calculations of pore volumes at the end of each nonlinear iteration. An iteratively coupled approach will produce the same results as a fully

coupled approach if both techniques use sufficiently tight convergence tolerances for iterations. Settari and Mourits,[5] and Fung, et al.[6] present examples of the iteratively coupled approach for multiphase flow. The primary attraction of the iteratively coupled approach is that it is very straightforward to couple an existing porous flow simulator with an existing geomechanics simulator. The primary drawback to the iteratively coupled approach is that the calculations may display a first order convergence rate in the nonlinear iterations and therefore may require a large number of iterations for difficult problems.

For the fully coupled approach, porous flow and displacement calculations are performed together, and the program's linear solver must handle both fluid flow variables and displacement variables. Tortike and Farouq Ali,[7] Li and Zienkiewicz,[8] and Lewis and Sukirman[9] have presented formulations of the fully coupled approach for poroelastic, multiphase flow. The primary attraction of the fully coupled approach is that it is the most stable approach of the three techniques and preserves second order convergence of nonlinear iterations. Drawbacks to the fully coupled approach are: it may be difficult to couple existing porous flow simulators and geomechanics simulators, it requires more code development than other techniques, and it can be slower than the explicit and iterative techniques on some problems.

The three techniques for coupling porous flow and geomechanics were incorporated into the same program so differences in the calculations could be attributed to the different techniques for coupling. If one were to compare three different programs each using a different technique for coupling, then it might be difficult to differentiate between differences due to coupling and differences due to basic algorithms in the separate programs. Comparison problems are presented for single-phase and three-phase flow problems involving poroelastic deformations. All techniques should produce the same results when using small time steps and tight convergence tolerances, so the choice between techniques is determined by ease of implementation, program availability, numerical stability, and computational efficiency.

A short review of the equations coupling porous flow and deformations is presented, followed by details of the algorithm for explicit coupling. Four problems are then presented and the results are compared using the three techniques. The first two problems are simple single-phase depletion problems that illustrate the role that stress and displacement boundary conditions play in porous flow calculations. The third problem is a single-phase depletion example where a soft reservoir is contained within a stiff nonpay region. The final problem is a three-phase, black-oil, five-spot pattern with a production well in one corner of the grid and a water injection well in the opposite corner. The coupling between geomechanics and fluid flow is fairly straightforward in problems 1, 2 and 4 and pressure histories for these runs can be reproduced by typical reservoir simulators with proper choices of compressibilities; however, problem 3 exhibits geomechanical effects that cannot be seen in reservoir simulations that do not include geomechanical calculations.

Coupled Flow and Deformation

For the problems in this paper, displacements enter the fluid flow equations through the calculation of reservoir pore volumes, and fluid pressures enter the displacement calculations through the stress/strain constitutive equations. A typical porous flow simulator expresses the pore volume for a grid block as

$$V_p = V_p^o\left[1 + c_r\left(p - p_o\right)\right] \quad \text{.....(1)}$$

where p is the fluid pressure and c_r is a compressibility-like term that must be entered by the user as part of the input data. However, for linear poroelastic calculations the pore volume for infinitesimal displacements may be expressed as

$$V_p = V_b^o\left[\varphi_o + \alpha\varepsilon_{kk} + \frac{1}{M}\left(p - p_o\right)\right] \quad \text{.....(2)}$$

where α and $1/M$ are Biot's parameters and Eq. 2 assumes expansion is positive. For the comparisons in this paper, α and $1/M$ are set equal to one and zero, respectively. For this choice of Biot's parameters, Eq. 1, a typical equation for flow simulators, expresses the pore volume in terms of the fluid pressure while Eq. 2 expresses the pore volume in terms of bulk strains, ε_{kk}. Flow simulators that are coupled to geomechanics programs may use an equation similar to Eq. 1 to approximate pore volume changes for the flow calculations and use an equation similar to Eq. 2 to calculate corrected pore volumes based upon reservoir deformations.

Logic that couples flow simulators to geomechanics programs must somehow account for the discrepancies between Eq. 1 and Eq. 2. Many coupling techniques will normally use a c_r term similar to that in Eq. 1 to enhance the coupling between flow calculations and displacement calculations. For explicitly coupled techniques, modified forms of Eq. 1 may be used to calculate pore volumes for those time steps where geomechanical updates are not performed. For iteratively coupled techniques, a c_r term may be included in the Jacobian for the flow equations, but Eq. 2 is always used to calculate pore volumes. For fully coupled techniques, a c_r term may be used in a preconditioning matrix for the flow equations when solving the linear system for flow variables and displacement variables.

The fluid pressure enters the deformation calculations through the linear poroelastic constitutive equation

$$\sigma_{ij} = \sigma_{ij}^o + \lambda\varepsilon_{kk}\delta_{ij} + 2\mu\varepsilon_{ij} - \alpha\left(p - p_o\right)\delta_{ij} \quad \text{.....(3)}$$

where tensile stresses are positive in Eq. 3. For the three-phase simulation included in this paper, the oil-phase pressure is used in Eqs. 1-3. For explicitly coupled and iteratively coupled techniques, the fluid pressure in Eq. 3 may be included in the equilibrium equation as a forcing function similar to the effects of a gravity head term. For a fully coupled technique, the fluid pressure in Eq. 3 generates a coefficient that must be

included in the Jacobian for the system of flow variables and displacement variables.

Explicit Coupling

The coupling algorithm for the explicit technique is described in more detail here because the algorithm uses both Eq. 2 and a modified form of Eq. 1 to calculate pore volumes for grid blocks during simulations. The iteratively coupled and fully coupled techniques may use a c_r term for the Jacobian or in a preconditioner to accelerate iterative calculations, but never actually use Eq. 1 to calculate pore volumes.

The explicit coupling algorithm allows a program to perform geomechanical calculations on a time scale that is different from the time scale for the flow calculations. This is very useful for subsidence problems because a large portion of the computational time in a simulation can be spent in performing geomechanical calculations. For many problems, fluid fronts may propagate or well changes may occur over very short time frames while subsidence may progress very slowly throughout the course of a simulation.

One can use Eqs. 1 and 2 to develop an algorithm for determining how often geomechanical calculations must be performed during a simulation. Let V_p^m be the pore volume for a grid block at time step m that was calculated using the geomechanical expression in Eq. 2. If the last geomechanical calculation was done for time step m, then for time step n > m, the pore volume in a grid block may be approximated by

$$\widetilde{V}_p^n = V_p^m + c_r^{est} V_p^o \left(p^n - p^m\right) \quad \text{.....(4)}$$

where p^n and p^m are the pressures for the grid block at time steps n and m, respectively. One may replace the V_p^o term in Eq. 4 by V_p^m; however, this does not change the accuracy of the approximation since terms at step m are constant in Eq. 4. Using V_p^m in place of V_p^o merely modifies the formula that one would develop for estimating values for the compressibility, c_r^{est}, at step m. Several techniques may be used to estimate compressibilities during a simulation. One approach derives analytical estimates of compressibilities using simple assumptions concerning stress and strain variations for a problem while a second approach uses pressure and pore volume changes between previous geomechanical updates during a simulation to estimate compressibilities. A third approach might calculate numerical estimates from the geomechanical equilibrium equations by calculating how variations in fluid pressures affect displacements. When estimating compressibilities, one may need to establish bounds for these estimates because values that are too large generate significant numerical errors and values that are too small give rise to oscillations or instabilities.

The explicitly coupled simulations in this paper use compressibilities in Eq. 4 that are derived from simple assumptions concerning stress and strain variations. For example, when a reservoir is deforming in the vertical direction and horizontal displacements are zero, uniaxial strain, then Eqs. 2 and 3 become approximately $\Delta V_p = V_b^o \Delta \varepsilon_{zz}$ and $\Delta \varepsilon_{zz} = \Delta p / (\lambda + 2\mu)$ when α=1 and 1/*M* = 0. So Eq. 2 and 3 may be combined as $\Delta V_p = V_b^o \Delta p / (\lambda + 2\mu)$. But Eq. 4 may be written as $\Delta \widetilde{V}_p^n = c_r^{est} \varphi_o V_b^o \Delta p$, which produces an estimate for c_r^{est} that is $\left[(\lambda + 2\mu)\varphi_o\right]^{-1}$. This may also be written in terms of the elastic modulus and Poisson's ratio as $(1+\nu)(1-2\nu)/\left[(1-\nu)\varphi_o E\right]$.

If one uses the geomechanical expression in Eq. 2 to calculate the pore volume V_p^n at step n, then one can compare V_p^n with $\widetilde{V}_p^n$ to determine errors in using Eq. 4 in place of Eq. 2. The relative error in pore volume for step n may be written as

$$E_{rel} = abs\left(\frac{\widetilde{V}_p^n - V_p^n}{V_p^n}\right) \quad \text{.....(5)}$$

During an explicitly coupled simulation, one does not have a value of E_{rel} for every time step, but only has values for those steps where geomechanical calculations are performed. It is natural to assume that the error in Eq. 5 is related to the relative change in pore volume since the last geomechanical update at step m, where the relative change in pore volume between steps m and n is approximated by

$$\left(\Delta V_p\right)_{rel} = abs\left(\frac{\widetilde{V}_p^n - V_p^m}{V_p^m}\right) \quad \text{.....(6)}$$

If one assumes that E_{rel} is proportional to $\left(\Delta V_p\right)_{rel}$ for those time steps where geomechanical calculations are not performed, then one can implement an algorithm that determines when displacements must be updated. One may estimate the parameter β in $E_{rel} \approx \beta \left(\Delta V_p\right)_{rel}$ as

$$\beta = \frac{E_{rel}}{\left(\Delta V_p\right)_{rel}} \quad \text{.....(7)}$$

where values of E_{rel} and $\left(\Delta V_p\right)_{rel}$ are determined from the two most recent time steps that included geomechanical updates. Prescribing a tolerance for E_{rel}, one may then use $\beta\left(\Delta V_p\right)_{rel}$ to determine when geomechanical updates need to be performed during subsequent time steps. The algorithm above is concerned with errors in pore volumes; however, similar logic may be applied to permeabilities if permeabilities change during a simulation. For the problems in this paper, the tolerance for E_{rel} is set to 0.001. The program also has options to specify updates for displacements after a prescribed number of time steps or after a presecribed pressure change since the

last update, but neither option was used for the problems in this paper.

Program Description

The three techniques for coupling flow and geomechanics are available in the program ACRES[10] (ARCO's Comprehensive REservoir Simulator). The program uses masses and a fluid pressure as primary variables for the flow equations and displacements as primary variables for deformations. The program contains IMPEM (IMplicit Pressure Explicit Mass) and implicit time stepping algorithms; however, all coupled runs are currently restricted to using the IMPEM technique for the flow calculations. The program uses finite differences (mixed finite elements with piecewise constant pressures) for the flow variables and finite elements for deformation variables. The program is capable of performing poroelastic and poroplastic calculations for black-oil and fully compositional applications. The displacement calculations use trilinear basis functions with eight Gaussian integration nodes for forming the stiffness matrix and a single integration node for integrating the fluid pressure in the equilibrium equation.

Comparison Problems

Four problems are used to compare the three techniques for coupling porous flow and geomechanics. The first two problems are simple single-phase depletion problems that illustrate the role that stress and displacement boundary conditions play in porous flow calculations. The third problem is a single-phase depletion example where a soft reservoir is contained within a stiff nonpay region. The final problem is a three-phase, black-oil, five-spot pattern with a production well in one corner of the grid and a water injection well in the opposite corner. Biot's parameters α and $1/M$ are set equal to one and zero, respectively, for all problems. All stresses described below are compressive and represent total stresses for the systems (include forces for fluid and solid).

All problems in this paper use a nonlinear convergence tolerance of 0.01 for volume errors, and a relative residual reduction tolerance of 0.01 for linear iterations, unless stated otherwise. The volume error is expressed as $(V_f-V_p)/V_p$ and the maximum is calculated for all grid blocks, where V_f and V_p are the fluid and pore volumes for a cell, respectively. All computing times presented in this paper are for a 700 Mhz Intel Mobile Pentium III.

Problems 1 and 2. Problems 1 and 2 are identical in description except problem 1 enforces zero displacement boundary conditions at the vertical faces of the grid and problem 2 applies constant horizontal stresses at the vertical faces of the grid. **Figs. 1a and 1b** show the stress and displacement boundary conditions for the two problems.

The grid is 11 x 11 x 10 with $\Delta x=\Delta y=200$ ft in the horizontal directions and $\Delta z=20$ ft in the vertical direction. The top of the grid is at a depth of 6000 ft, the initial in situ reservoir porosity is 20%, and the reservoir permeabilities are 50 md and 5 md in the horizontal and vertical directions, respectively. The fluid is single phase with a formation volume factor of 1.0, a viscosity of 1 cp, a fluid density of 62.4 lbm/ft^3, and zero fluid compressibility. The initial fluid pressure is 3000 psi at a depth of 6000 ft.

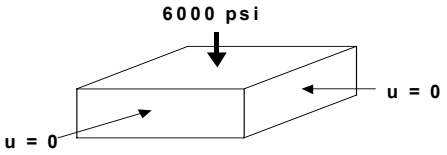

Fig. 1a – Constrained displacements for problem 1

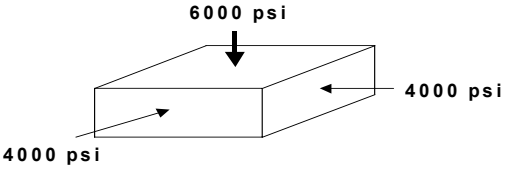

Fig. 1b – Unconstrained displacements for problem 2

The elastic modulus is 1 x 10^4 psi, Poisson's ratio is 0.3, and the initial in situ solid density (solid material without pores) is 2.7 gm/cm^3. Initial horizontal stresses are 4000 psi over the entire reservoir depth while the initial vertical stress is 6000 psi at 6000 ft with a vertical stress gradient of 1.0231 psi/ft throughout the reservoir. The bottom of the grid has a zero vertical displacement constraint and all faces of the grid have zero tangential stresses. Both problems apply a normal stress of 6000 psi at the top of the grid while problem 1 enforces zero normal displacements at the four vertical faces of the grid and problem 2 applies a normal stress of 4000 psi at these same faces. Assuming uniaxial strain behavior for problem 1 and constant total stresses for problem 2, the explicitly coupled simulations in this paper use constant values of 3.71 x 10^{-4} psi^{-1} and 6.00 x 10^{-4} psi^{-1} for the compressibility in Eq. 4.

A vertical well with a wellbore radius of 0.25 ft is completed in the center of the pattern in all ten layers of the grid, cells (6,6,1-10). The well is produced at a rate of 15,000 b/d for 500 days with a time step size of 10 days. No flow boundary conditions are assumed for the fluid at all faces of the grid.

Fig. 2 shows average pore-volume-weighted reservoir pressures for problems 1 and 2 using the three different techniques. All techniques produced nearly identical results for each problem. Fig. 2 shows how geomechanical stress or displacement boundary conditions influence the pressure response in the reservoir. Problem 2 shows much less pressure drop than problem 1 because of the support provided by the constant stress boundary conditions on the sides of the reservoir.

The runtime information for problems 1 and 2 are displayed in Tables 1 and 2. The column for iterations is the number of nonlinear iterations during a simulation. The explicitly coupled technique is faster than the other two techniques for this problem because it performs a small number of updates for the displacements when using an E_{rel} tolerance of 0.001.

The explicitly coupled technique performs 18 and 15 updates for the displacements for problems 1 and 2, respectively.

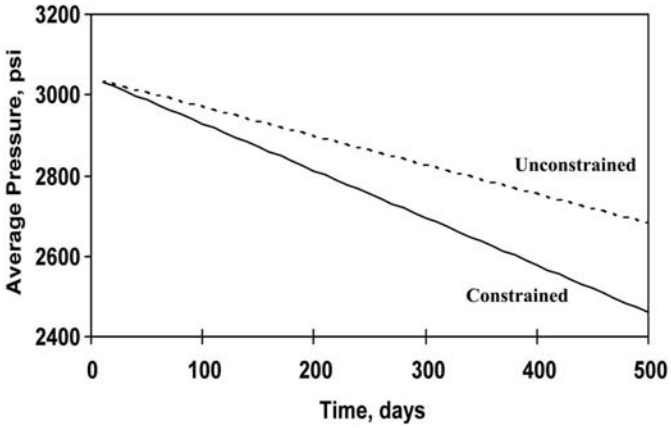

Fig. 2 – Average pressures for problems 1 and 2

Technique	*CPU Time*	*Time Steps*	*Iterations*
Explicit	**8.0 seconds**	**50**	**53**
Iterative	**10.7**	**50**	**51**
Full	**13.3**	**50**	**51**

Table 1 – Runtime information for problem 1

Technique	*CPU Time*	*Time Steps*	*Iterations*
Explicit	**7.8 seconds**	**50**	**53**
Iterative	**10.7**	**50**	**52**
Full	**12.4**	**50**	**51**

Table 2 – Runtime information for problem 2

Fig. 3 shows the subsidence at the top of the reservoir at the well for problems 1 and 2. The two problems produce similar displacements at early times, but the problems deviate substantially at later times. The change in subsidence in Fig. 3 is not a linear function of the average pressure drop in Fig. 2 until later in the run when a pseudo-steady state is reached for the pressure behavior.

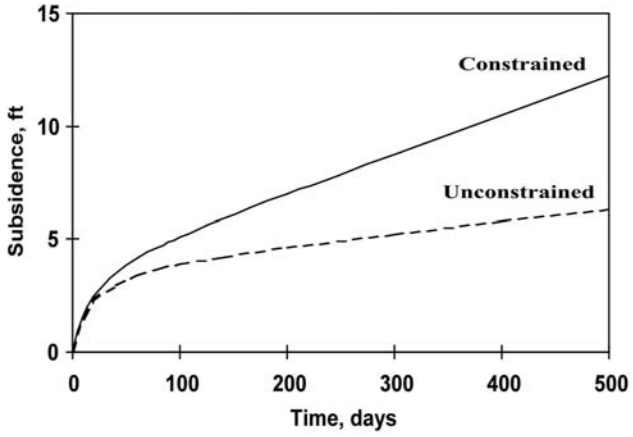

Fig. 3 – Subsidence for problems 1 and 2

The total subsidence for problem 1 is 12.2 ft after 500 days. This corresponds to an average vertical strain of 6.1%, which is very large considering that the calculations are based upon infinitesimal strain assumptions. Even though the pressures in Fig. 2 are based upon calculations using infinitesimal strains; it is expected that the results should not change substantially if the calculations are repeated using a finite strain formulation. Based upon a simple uniaxial strain analysis, a finite strain simulation should predict a final average pressure for the constrained case that is about 10 psi larger than the result shown in Fig. 2.

Problem 3. Problem 3 is modeled after a problem presented by M. Gutierrez and R.W. Lewis.[11] Problem 3 includes a soft productive reservoir that is contained within a stiff nonpay region as shown in **Fig. 4**. Problem 3 displays a geomechanical effect at the boundary of the reservoir that cannot be seen in reservoir simulations that do not include geomechanical calculations. For this problem, geomechanical effects cause the fluid pressures to increase at the boundary of the reservoir during the initial stages of depletion.

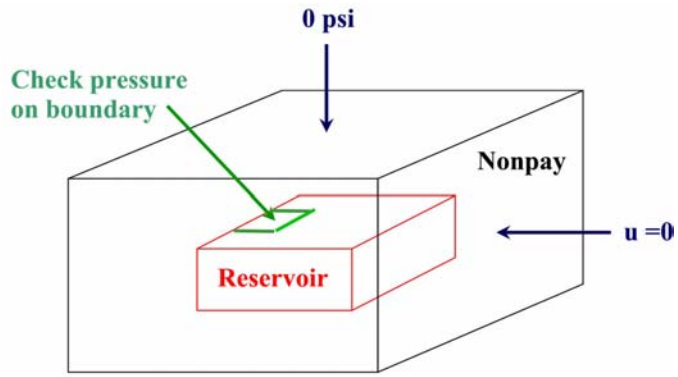

Fig. 4 – Reservoir and nonpay regions for problem 3

The grid is 21 x 21 x 12 and includes both the reservoir and nonpay regions. Grid block lengths in the x-direction are 4000 ft each for the first 5 grid blocks, 2000 ft each for the next 11 grid blocks, and 4000 ft each for the last 5 grid blocks. Grid block lengths for the y-direction are half the corresponding values in the x-direction. The top of the grid is at a depth of 0 ft and the thicknesses in the vertical direction are 4000, 3000, 2000, 800, and 200 ft for the first 5 layers that represent the overburden. The next five layers have thicknesses of 50 ft each and represent the reservoir. The last two layers have thicknesses of 100 ft each and represent the underburden. The horizontal and vertical permeabilities are 100 and 10 md, respectively, in the reservoir, cells (6-16,6-16,6-10). Permeabilities are zero in the nonpay region. The initial in situ porosity is 25% in both the reservoir and nonpay regions.

The fluid is single phase with a formation volume factor of 1.0 at 14.7 psi, a viscosity of 1 cp, a fluid density of 62.4 lbm/ft^3 at 14.7 psi, and fluid compressibility of 3 x 10^{-6} psi^{-1}. A nonzero fluid compressibility is used for this problem because a zero fluid compressibility makes the porous solid incompressible in the nonpay region. The initial fluid pressure is 14.7 psi at the surface.

The elastic moduli are 1 x 10^4 psi in the reservoir and 1 x 10^6 psi in the nonpay region, Poisson's ratio is 0.25 everywhere, and the initial in situ solid density (solid material without pores) is 2.7 gm/cm^3. The initial vertical stress is 0 psi at the surface with a vertical stress gradient of 0.9869 psi/ft

throughout the grid, and initial horizontal stresses are equal to half of the vertical stress. The bottom and sides of the grid have zero normal displacement constraints and all faces of the grid have zero tangential stresses. Assuming uniaxial strain behavior for this problem, the explicitly coupled simulation uses values of 3.33×10^{-4} psi^{-1} and 3.33×10^{-6} psi^{-1} for the compressibility in Eq. 4 in the reservoir and nonpay regions, respectively.

A vertical well with a wellbore radius of 0.25 ft is completed in the center of the reservoir in all five layers, cells (11,11,6-10). The well is produced at a rate of 50,000 stb/d for 4000 days with a time step size of 20 days for the first 400 days, followed by time steps of 200 days stopping at 4000 days. Smaller time steps are taken at the beginning of the run to produce an accurate solution for the pressure increase at the reservoir boundary. Iteratively coupled and fully coupled techniques should be able to produce accurate results using the time steps specified for this problem, but explicitly coupled techniques may require time steps that are smaller than 20 days because of time discretization errors that arise due to the explicit coupling.

Fig. 5 shows average pore-volume-weighted pressures in the reservoir (excluding nonpay region) using the three different techniques. The three techniques produce significantly different results in Fig. 5 after the time step size increases from 20 days to 200 days.

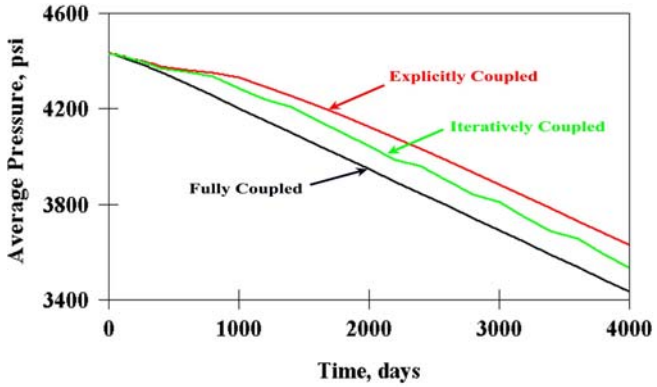

Fig. 5 – Average reservoir pressures for problem 3

The three techniques also predict large differences in pressures at the boundary of the reservoir at early times. The iteratively coupled technique requires a tighter tolerance on the nonlinear iterations and the explicitly coupled technique requires smaller time steps to reproduce the fully coupled results. For this problem, the iteratively coupled technique requires a nonlinear volume error tolerance of 0.0001 and the explicitly coupled technique requires a time step size of about one day. One can improve the explicitly coupled results by using a smaller value of estimated compressibility for this problem; however, values that are too small will produce oscillations in well pressures.

Fig. 6 shows the subsidence at the top of the reservoir and at the surface for all three techniques. The explicitly coupled results included in Fig. 6 use a time step size of one day for the simulation. The original explicitly coupled results using time step sizes of 20 days and 200 days did not agree well with the results in Fig. 6 predicting a final subsidence of 6.47 ft at the top of the reservoir. The final subsidence in Fig. 6 at the top of the reservoir is 7.76 ft.

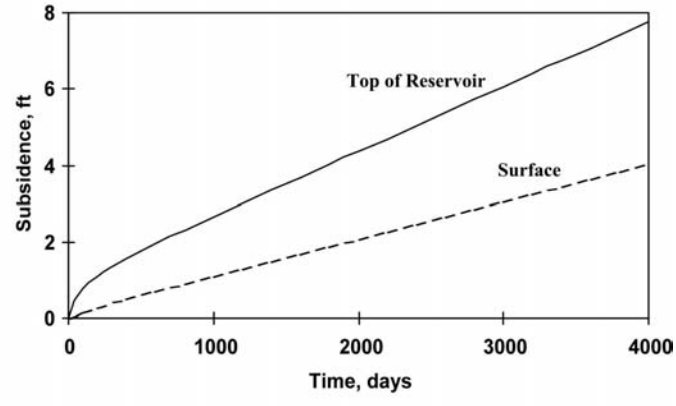

Fig. 6 – Subsidence for problem 3

Fig. 7 shows the pressure behavior at the boundary of the reservoir in cell (6,11,6). Initially the reservoir pressure increases as the reservoir is depleted because some of the vertical load that was supported at the center of the reservoir is transferred to the edges of the reservoir. This pressure increase cannot be observed in a reservoir depletion problem that does not include geomechanical calculations. The iteratively coupled results in Fig. 7 use a volume error tolerance of 0.0001, and the explicitly coupled results use a time step size of one day updating displacements every time step.

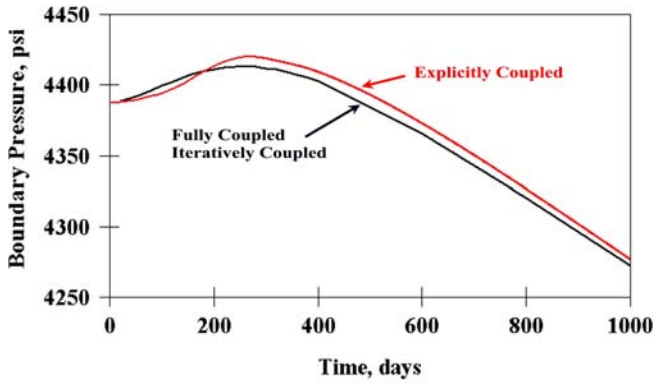

Fig. 7 – Pressure at boundary of reservoir for problem 3

The runtime results for problem 3 are shown in Table 3. The explicitly coupled technique is much slower than the other two techniques for this problem because it requires much smaller time step sizes. The fully coupled and iteratively coupled techniques also exhibit time discretization errors, but time discretization errors play a much larger role for the explicitly coupled technique. The iteratively coupled technique is slower than the fully coupled technique because the iteratively coupled technique requires a large number of nonlinear iterations for convergence. Also, the iteratively coupled technique exhibits only a first order rate of convergence for the nonlinear iterations because of the sequential nature of updating the flow and displacement equations.

Technique	*CPU Time*	*Time Steps*	*Iterations*
Explicit	**51.8 minutes**	**4000**	**4000**
Iterative	**6.9**	**38**	**449**
Full	**4.3**	**38**	**38**

Table 3 – Runtime information for problem 3

Problem 4. Problem 4 is a three-phase, five-spot with a water injection well in one corner of the grid and a production well in the diagonally opposite corner of the grid. The production rate is larger than the injection rate so the reservoir pressure decreases throughout the simulation.

The grid for problem 4 is displayed in **Fig. 8** showing water saturations at the end of 25 years. The grid is 21 x 21 x 11 with $\Delta x=\Delta y=60$ ft in the horizontal directions and $\Delta z=20$ ft in the vertical direction. The top of the grid is at a depth of 4000 ft, and the initial in situ reservoir porosity is 30%. Reservoir permeabilities vary by layer with horizontal permeabilities equal to 5, 100, 20, 20, 20, 100, 20, 20, 100, 20, and 20 md, respectively. Vertical permeabilities are 0.01 times horizontal permeabilities. Two–phase relative permeabilities and capillary pressures are listed in Tables 4 and 5, and Stone 2 is used for three-phase relative permeabilities.[12]

Water has a formation volume factor of 1.0 at 14.7 psi, a viscosity of 1 cp, a fluid density of 62.4 lbm/ft^3 at 14.7 psi, and fluid compressibility of 3 x 10^{-6} psi^{-1}. The oil and gas densities at the surface are 56.0 lbm/ft^3 and 57.0 lbm/mcf, respectively. Pressure-dependent oil and gas properties are listed in Table 6.

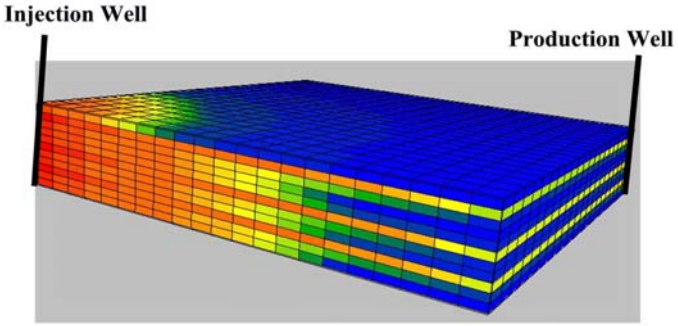

Fig. 8 –Water saturations after 25 years for problem 4

The initial reservoir pressure is 3010 psi at 4010 ft and initial fluid saturations are 20%, 80% and 0% for water, oil and gas, respectively. The oil is initially undersaturated with a bubble-point pressure of 3000 psi and an oil compressibility of 10^{-5} psi^{-1} in all layers.

The elastic modulus is 5 x 10^4 psi, Poisson's ratio is 0.35, and the initial in situ solid density (solid material without pores) is 2.7 gm/cm^3. The initial vertical stress is 4000 psi at the top of the reservoir with a vertical stress gradient of 0.9256 psi/ft throughout the grid and initial horizontal stresses are equal to half of the vertical stress. The bottom and sides of the grid have zero normal displacement constraints and all faces of the grid have zero tangential stresses. Assuming uniaxial strain behavior for this problem, the explicitly coupled simulation uses a value of 4.15 x 10^{-5} psi^{-1} for compressibility in Eq. 4.

Vertical wells are completed in diagonally opposite corners of the grid in all 11 layers. The water injector has a prescribed rate of 500 stb/d (¼ of the well's total rate), and the production well has a prescribed liquid rate of 750 stb/d (¼ of the well's total rate) with a limiting bottomhole pressure of 500 psi. Wellbore radii of 0.069 ft (instead of 0.25 ft) are used to represent wells of radii 0.25 ft that are at the corners of the grid blocks,[13] and a multiplying factor of 0.25 is used for the wellbore constants since only ¼ of a well's production is being simulated in the pattern. Simulations are performed for 25 years using time step sizes that are controlled by stability considerations for the IMPEM technique.

The three techniques produce nearly identical results for problem 4. **Fig. 9** shows average pore-volume-weighted, oil-phase pressures and subsidence in the center of the pattern at the top of the reservoir. **Fig. 10** shows the wellbore pressure, gas/oil ratio, and water/oil ratio at the production well.

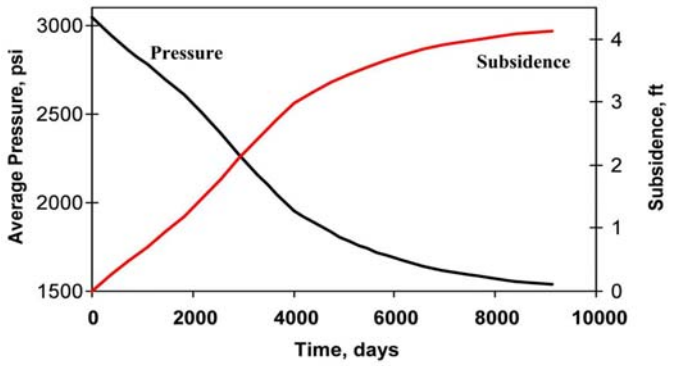

Fig. 9 – Average pressure and subsidence for problem 4

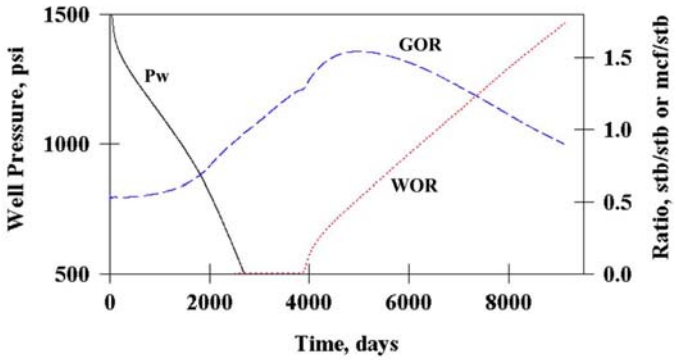

Fig. 10 – Production history for problem 4

The runtime information for problem 4 is displayed in Table 7. The explicitly coupled technique is much faster than the other two techniques for this problem because it performs a small number of geomechanical updates during the simulation. The explicitly coupled technique requires only 33 updates for displacements throughout the simulation. A minimum of 25 updates are required because displacements are printed each year during the simulation. The iteratively coupled and fully coupled techniques would perform better for this problem if they were combined with the implicit time stepping option in

the program, rather than with the IMPEM option, but it is expected that the explicitly coupled option would still be the best option because few geomechanical updates are required.

Technique	*CPU Time*	*Time Steps*	*Iterations*
Explicit	**9.0 minutes**	**3324**	**3325**
Iterative	**40.6**	**3326**	**3326**
Full	**47.5**	**3326**	**3326**

Table 7 – Runtime information for problem 4

A run was performed without geomechanical calculations using a value of 4.15 x 10^{-5} psi^{-1} for c_r in Eq. 1 and the results reproduced the pressure and fluid histories in Figs. 9 and 10. The simulation without geomechanical calculations took 7.2 minutes; so for this problem, geomechanical calculations add only 25% to the overall computational time for the model when using the explicitly coupled technique.

Conclusions

Explicitly coupled, iteratively coupled, and fully coupled techniques have been applied to four sample problems. The three techniques produce nearly identical results on problems 1, 2, and 4 using the same time step sizes and the same convergence tolerances. Problem 3 involves geomechanical effects that are not present in the other three problems and the three techniques initially produced different results for this problem; however, all three techniques produced similar results when a tight tolerance was used for the nonlinear iterations for the iteratively coupled technique, and when small time steps were used for the explicitly coupled technique. All problems in this paper are described in detail so the results presented here may be used for comparison with other geomechanical/porous flow simulators.

The three coupling techniques produce similar results and one's selection of a technique is determined by ease of implementation, program availability, numerical stability, and computational efficiency. No technique worked best on all four problems presented in this paper. The fully coupled technique worked best for problem 3 running twelve times faster than the explicitly coupled technique, and the explicitly coupled technique worked best for problem 4 running five times faster than the fully coupled technique.

Acknowledgements

BP provided a copy of ACRES to the University of Texas at Austin for running the comparisons in this paper. The authors would like to acknowledge the support of DOE, NSF, NGOTP, and the Industrial Affiliates of the Center for Subsurface Modeling at the University of Texas at Austin. Sandia is a multiprogram laboratory operated by Sandia Corporation, a Lockheed Martin Company, for the United States Department of Energy under contract DE-AC04-94AL85000.

Nomenclature

c_r = reservoir compressibility, Lt^2/m, psi^{-1}
E = elastic modulus, m/Lt^2, psi
E_{rel} = relative difference in pore volumes
M = Biot's poroelastic parameter, m/Lt^2, psi
p = fluid pressure, m/Lt^2, psi
p_o = initial fluid pressure, m/Lt^2, psi
V_b^o = initial grid block volume, L^3, ft^3
V_p = pore volume, L^3, ft^3
$\widetilde{V}_p$ = pore volume estimate from pressure equation, L^3, ft^3
V_p^o = initial pore volume, L^3, ft^3
α = Biot's poroelastic parameter, dimensionless
δ_{ij} = Kronecker delta, dimensionless
Δ = change in a variable, dimensionless
ε_{ij} = strain, expansion is positive, dimensionless
ε_{kk} = volumetric strain, dimensionless
λ = Lame constant, m/Lt^2, psi
μ = Lame constant, m/Lt^2, psi
ν = Poisson's ratio, dimensionless
σ_{ij} = total stress, tension is positive, m/Lt^2, psi
σ_{ij}^o = initial total stress, m/Lt^2, psi
φ_o = initial porosity, dimensionless

References

1. Minkoff, S., Stone, C., Arguello, J., Bryant, S., Eaton, J., Peszynska, M. and Wheeler, M., "Staggered in Time Coupling of Reservoir Flow Simulation and Geomechanical Deformation: Step 1 --- One-Way Coupling," paper SPE 51920 presented at the 1999 SPE Reservoir Simulation Symposium, Houston, Feb. 14-17.
2. Settari, A. and Walters, D.A., "Advances in Coupled Geomechanical and Reservoir Modeling With Applications to Reservoir Compaction," paper SPE 51927 presented at the 1999 SPE Reservoir Simulation Symposium, Houston, Feb.14-17.
3. Minkoff, S., Stone, C., Arguello, J., Bryant, S., Eaton, J., Peszynska, M. and Wheeler, M., "Coupled Geomechanics and Flow Simulation for Time-Lapse Seismic Modeling," 69th Annual International Meeting of Soc. of Expl. Geophys. (1999) 1667-1670.
4. Minkoff, S., Stone, C., Bryant, S., Peszynska, M. and Wheeler, M., "A Two-way, Staggered-in-time, Loose Coupling Algorithm for Sophisticated Fluid Flow and Geomechanical Deformation Modeling," submitted in 2002 to Journal of Petroleum Science and Engineering.
5. Settari, A. and Mourits, F.M., "Coupling of geomechanics and reservoir simulation models," Comp. Methods and Advances in Geomech., Siriwardane and Zeman, (eds.), Balkema, Rotterdam (1994) 2151-2158.
6. Fung, L.S.K., Buchanan, L. and Wan, R.G., "Coupled Geomechanical-thermal Simulation for Deforming Heavy-oil Reservoirs," J. Cdn. Pet. Tech. (April 1994) 22.
7. Tortike, W.S., and Farouq Ali, S.M., "A Framework for Multiphase Nonisothermal Fluid Flow in a Deforming Heavy Oil Reservoir," paper SPE 16030 presented at the 1987 SPE Reservoir Simulation Symposium, San Antonio, Feb. 1-4.
8. Li, X. and Zienkiewicz, O.C., "Multiphase Flow in Deforming Porous Media and Finite Element Solutions," Computers and Structures (1992) 45, 211.
9. Lewis, R.W., and Sukirman, Y., "Finite Element Modelling of Three-Phase Flow in Deforming Saturated Oil Reservoirs," Intl. J. for Num. and Anal. Methods in Geomech.(1993) 17, 577.
10. ARCO Reservoir Simulator Development, "Appendix 30: Poroelastic Calculations," ACRES Reference Manual, Internal ARCO Document, ARCO, Plano, TX, 1999.

11. Gutierrez, M. and Lewis, R.W., "The Role of Geomechanics in Reservoir Simulation," paper SPE/ISRM 47392 presented at the 1998 SPE/ISRM Eurock Conference, Trondheim, July 8-10.
12. Stone, H.L., "Estimation of Three-Phase Relative Permeability and Residual Oil Data," J. Can. Pet. Tech. (1973) 12, 53.
13. Kuniansky, J. and Hillestad, J.G., "Reservoir Simulation Using Bottomhole Pressure Boundary Conditions," SPEJ (Dec. 1980) 473.

Metric Conversion Factors

bbl x 1.589 874	E-01	=	m^3
cp x 1.0*	E-03	=	Pa s
ft x 3.048*	E-01	=	m
lbm x 4.535924	E-01	=	kg
mcf x 2.831 685	E+01	=	m^3
md x 9.869 233	E-04	=	μm^2
psi x 6.894 757	E+00	=	kPa
psi^{-1} x 1.450 377	E-01	=	kPa^{-1}

*Conversion factor is exact.

Sw	Krw	Krow	Pwc
0.2	0.0	0.5102	6.4
0.25	0.0039	0.4133	5.6
0.3	0.0156	0.3266	4.9
0.35	0.0352	0.2500	4.2
0.4	0.0625	0.1837	3.6
0.45	0.0977	0.1276	3.0
0.5	0.1406	0.0816	2.5
0.55	0.1914	0.0459	2.0
0.6	0.2500	0.0204	1.6
0.65	0.3164	0.0051	1.2
0.7	0.3906	0.0	0.9
0.8	0.5625	0.0	0.4
0.9	0.7656	0.0	0.1
1.0	1.0	0.0	0.0

Table 4 – Water/oil data for problem 4

Sw+So	Krog	Krg	Pgc
0.2	0.0	0.6303	3.2
0.25	0.0	0.5511	2.8
0.3	0.0	0.4772	2.5
0.35	0.0026	0.4086	2.1
0.4	0.0104	0.3454	1.8
0.45	0.0234	0.2874	1.5
0.5	0.0416	0.2348	1.3
0.55	0.0651	0.1875	1.0
0.6	0.0937	0.1455	0.8
0.65	0.1275	0.1089	0.6
0.7	0.1666	0.0775	0.5
0.75	0.2108	0.0514	0.3
0.8	0.2709	0.0307	0.2
0.85	0.3149	0.0153	0.1
0.9	0.3748	0.0052	0.0
0.95	0.4398	0.0004	0.0
0.97	0.4673	0.0	0.0
1.0	0.5102	0.0	0.0

Table 5 – Gas/oil data for problem 4

Pressure psi	B_o rvb/stb	B_g rvb/mcf	R_s mcf/stb	μ_o cp	μ_g cp
300.00	1.0663	10.2582	.0610	1.5	.02
600.00	1.0931	4.9878	.1161	1.5	.02
900.00	1.1173	3.2461	.1681	1.5	.02
1200.00	1.1408	2.3855	.2197	1.5	.02
1600.00	1.1718	1.7522	.2894	1.5	.02
2000.00	1.2030	1.3838	.3608	1.5	.02
2400.00	1.2346	1.1479	.4342	1.5	.02
2800.00	1.2667	.9876	.5102	1.5	.02
3000.00	1.2843	.9221	.5521	1.5	.02
3200.00	1.2996	.8743	.5889	1.5	.02
3600.00	1.3334	.7921	.6708	1.5	.02
4000.00	1.3683	.7312	.7561	1.5	.02
4500.00	1.4137	.6763	.8685	1.5	.02

Table 6 – Pressure dependent oil and gas data for problem 4